PLoS one

Anion-Sensitive Regions of L-Type CaV1.2 Calcium Channels Expressed in HEK293 Cells

Norbert Babai[1], Nataly Kanevsky[2], Nathan Dascal[2], George J. Rozanski[3], Dhirendra P. Singh[1], Nigar Fatma[1], Wallace B. Thoreson[1]*

1 Department of Ophthalmology & Visual Science, University of Nebraska Medical Center, Omaha, Nebraska, United States of America, 2 Department of Physiology and Pharmacology, Sackler School of Medicine, Tel Aviv University, Ramat Aviv, Israel, 3 Department of Cellular & Integrative Physiology, University of Nebraska Medical Center, Omaha, Nebraska, United States of America

Abstract

L-type calcium currents (I_{Ca}) are influenced by changes in extracellular chloride, but sites of anion effects have not been identified. Our experiments showed that CaV1.2 currents expressed in HEK293 cells are strongly inhibited by replacing extracellular chloride with gluconate or perchlorate. Variance-mean analysis of I_{Ca} and cell-attached patch single channel recordings indicate that gluconate-induced inhibition is due to intracellular anion effects on Ca^{2+} channel open probability, not conductance. Inhibition of CaV1.2 currents produced by replacing chloride with gluconate was reduced from ~75%–80% to ~50% by omitting β subunits but unaffected by omitting $\alpha_2\delta$ subunits. Similarly, gluconate inhibition was reduced to ~50% by deleting an α1 subunit N-terminal region of 15 residues critical for β subunit interactions regulating open probability. Omitting β subunits with this mutant α1 subunit did not further diminish inhibition. Gluconate inhibition was unchanged with expression of different β subunits. Truncating the C terminus at AA1665 reduced gluconate inhibition from ~75%–80% to ~50% whereas truncating it at AA1700 had no effect. Neutralizing arginines at AA1696 and 1697 by replacement with glutamines reduced gluconate inhibition to ~60% indicating these residues are particularly important for anion effects. Expressing CaV1.2 channels that lacked both N and C termini reduced gluconate inhibition to ~25% consistent with additive interactions between the two tail regions. Our results suggest that modest changes in intracellular anion concentration can produce significant effects on CaV1.2 currents mediated by changes in channel open probability involving β subunit interactions with the N terminus and a short C terminal region.

Introduction

L-type Ca^{2+} channels are involved in many vital functions including contraction of skeletal, smooth, and cardiac muscle; release of neurohormones and neurotransmitters; and gene expression [1–4]. They can be regulated by many different mechanisms [1,5–7]. One poorly understood mechanism involves the effects of anions on I_{Ca}. Replacing Cl^- with various substituting anions influences many Ca^{2+}-mediated processes including contractility of cardiac and skeletal muscle, hormone secretion, and neurotransmitter release [8–16]. An important contributor to these anion effects is the modulation of L-type Ca^{2+} currents (I_{Ca}) [8–10,17,18]. Large reductions in extracellular chloride produced by replacing Cl^- with gluconate or perchlorate can substantially inhibit I_{Ca} [8,18]. Replacing a small amount of Cl^- with gluconate can also produce significant inhibitory effects [8,18] but small concentrations of perchlorate can have stimulatory effects [13,14,16]. The inhibition of I_{Ca} produced by replacing chloride with gluconate and the enhancement of I_{Ca} caused by low concentrations of perchlorate have both been shown to be due to the actions of anions at intracellular sites which alter the open probability of Ca^{2+} channels [16,17].

Chloride and other anions influence the structure and activity of many different proteins including opsins [19], intracellular Ca^{2+} channels [20], hemoglobin [21,22], albumin [23], PDZ domains [24], K^+ channels [25,26], kainate receptors [27], serine/threonine kinases [28–30], and G proteins [31]. Anion effects on protein function typically involve binding to positively charged lysine or arginine residues. In the present study, we expressed different subunit combinations and CaV1.2 mutant channels in HEK293 cells to analyze channel regions responsible for the anion sensitivity of L-type Ca^{2+} channels. We identified two anion-sensitive regions of L-type Ca^{2+} channels: 1) a short region of the C terminus in which a pair of neighboring arginine residues is particularly important and 2) interactions between accessory β subunits and a short region of the N terminus. Consistent with previous reports, we found that anions act inside the cell to modulate Ca^{2+} channel open probability and low anion concentrations can produce significant effects on I_{Ca}. These results suggest that modest, physiologically-attainable changes in the intracellular levels of chloride or other anions can influence the activity of L-type Ca^{2+} channels by actions at multiple channel regions and thus potentially influence Ca^{2+}-dependent processes in many different tissues throughout the body.

Materials and Methods

Ethics Statement

All animal procedures were approved by University of Nebraska Medical Center Institutional Animal Care and Use Committee, and conducted according to the *Guide for the Care and Use of Laboratory Animals*, published by the National Institutes of Health (NIH Publication No. 85-23, Revised 1996).

HEK293 cells were grown in DMEM supplemented with 10% fetal bovine serum (FBS) and 50 U/ml gentamicin and maintained at 37°C in a humidified incubator with 5% CO_2. Upon nearing confluence, cells were dissociated enzymatically with trypsin-EDTA and plated overnight on 13mm diameter plastic cover-slips (NUNC, Rochester, NY USA) in 35×10mm tissue culture dish (Falcon, Franklin Lakes, NJ. USA). Cover-slips were transferred to 24 well tissue culture plates with 0.5 ml grown media without antibiotic and FBS (Falcon, Franklin Lakes, NJ. USA) and transiently transfected using Lipofectamine 2000 (Invitrogene, Carlsbad, CA). cDNA from the α1 subunit (1 μg) was cotransfected with one of the rat β subunits (1 μg) (i.e., β_{2a}, β_{1b}, β_3, or β_4) and the rat $\alpha_2\delta$ (1 μg) subunit. The α1 subunits used in this study were a short N-terminal isoform of CaV1.2 derived from rat brain [32] (M67515), a long N-terminal isoform of rabbit CaV1.2 derived from cardiac tissue [33] (X15539), and various mutants of rabbit CaV1.2. The Δ139/Δ1665 double mutant was constructed by cutting and ligating appropriate parts of the Δ139 and Δ1665 mutants. Details of the other CaV1.2 mutants are described elsewhere [33–36]. We co-transfected cells with enhanced green fluorescent protein (eGFP) (1 μg; Clontech, Cambridge, UK) as a marker plasmid. Transfected cells were incubated in transfection medium for 6–8 hrs. before replacing it with standard growth medium. Cells were used for recording 24–72 hrs. after transfection.

Cells were superfused at room temperature using a single-pass, gravity-fed perfusion system (1 ml/min) with an oxygenated medium containing (in mM): 130 NaCl, 5 KCl, 5 $BaCl_2$, 10 4-*N*-2-hydroxyethylpiperazine-*N*' 2-ethanesulfonic acid (HEPES), 10 glucose (pH 7.4). For anion replacement experiments, we replaced NaCl and KCl but not $BaCl_2$. Gluconate weakly chelates Ba^{2+} and calculations using WCabuf (G. Droogmans, Leuven, Belgium) indicate that the free Ba^{2+} concentration is reduced by gluconate replacement from 5 mM to 4.34 mM. However, in control experiments, we found that reducing Ba^{2+} to 4.34 mM did not significantly reduce CaV1.2 currents ($-2.7\pm2.2\%$, N = 7, P = 0.996).

Whole cell recordings were obtained using patch electrodes pulled from borosilicate pipettes (1.2 mm outer diameter, 0.95 mm inner diameter, with internal filament) using a Narishige PP-830 vertical puller. The recording pipettes had tips of 1–2 μm outer diameter (R = 7–10 MΩ) and were filled with a solution containing (in mM): 125 CsCl, 10 tetraethyl ammonium chloride (TEACl), 10 HEPES, 3 ethylene glycol *bis* (β-aminoethyl ether) N, N, $\dot{N}$, $\dot{N}$-tetraacetic acid (EGTA), 1 ATP, 0.5 GTP, 3 $MgCl_2$, 1 $CaCl_2$ (pH 7.2). The low Cl^- pipette solution contained (in mM): 125 Cs gluconate, 10 TEACl, 10 HEPES, 3 EGTA, 1 ATP, 0.5 GTP, 3 $MgCl_2$, 1 $CaCl_2$ (pH 7.2). The reference electrode was connected to the bath by a 3 M KCl/agar bridge. With the agar bridge in place, the liquid junction potential changed by ≤1 mV when chloride in the bathing medium was replaced with gluconate.

HEK cells were voltage clamped at -70 mV using an Axopatch 200B or Multiclamp amplifier (Axon Instruments, Foster City, CA). The barium current (I_{Ba}) was typically recorded with a ramp voltage protocol (-90 to $+60$ mV, 0.5 mV/ms). I_{Ba} was fit with a Boltzmann function adjusted for driving force. The fitting region extended from baseline to 10 mV beyond the peak inward current. Current/voltage relationships measured with ramp protocols matched current/voltage relationships determined from steady state currents evoked by depolarizing steps (100 ms, 10 mV increments; Fig. S1). Currents were acquired using PClamp 9.2 with a Digidata 1322 interface (Axon Instruments). Currents were leak-subtracted *post-hoc* or by using P/8 protocols.

Single ventricular myocytes were dissociated from isolated, perfused rat hearts by a collagenase digestion procedure described previously [37]. Dissociated myocytes were suspended in DMEM and stored in an incubator at 37°C. Aliquots of myocytes to be studied were transferred to a cell chamber mounted on the stage of an inverted microscope and superfused with an external solution containing (in mM): 138 NaCl; 4 CsCl; 0.5 $MgCl_2$; 1.8 $CaCl_2$; 10 glucose; 5 HEPES (pH 7.4).

For measurements of I_{Ca} from ventricular myocytes, currents were evoked by 300 ms depolarizing pulses to test potentials between -40 and $+60$ mV (0.2 Hz). The holding potential in all experiments was -80 mV and 100 ms prepulse to -50 mV was applied to inactivate the fast Na^+ current. At each test potential the amplitude of I_{Ca} was measured as the difference between the peak inward current and the current level at the end of the depolarizing clamp pulse. Data were normalized as current densities by dividing measured current amplitude by whole-cell membrane capacitance (pA/pF).

For mean/variance analysis of single channel current amplitudes from CaV1.2 channels expressed in HEK293 cells, we applied 100 test pulses (5 ms) from -70 to $+50$ mV. For these experiments, currents were filtered at 5 kHz and access resistance was compensated 80–90%. For P/200 subtraction of passive and capacitative currents, we summed two trials involving 100 tests pulses of 1.2 mV amplitude recorded immediately before and after the test pulse series. The mean amplitude and variance was determined at each time point during the tail current. The mean/variance relationship was fit with a parabolic function:

$$V = iI - I^2/N + A$$

where I = mean whole cell current amplitude, i = single channel current amplitude, N = channel number, A = offset, and V = variance.

Cell-attached patch recordings of single CaV1.2 channels were obtained using pipettes coated with Sylgard (Dow Corning, Midland, MI) and filled with 82 mM $BaCl_2$. Recordings were low pass filtered with a cutoff frequency of 2 kHz and digitized at 50 μs/sample. In the cell-attached patch configuration, the transmembrane voltage across the patch is a sum of the cell membrane potential and voltage applied by the amplifier. Using gramicidin (5 μg/ml) as a perforating agent along with a pipette solution containing (in mM): 98 KCH_3SO_4; 44 KCl; 3 NaCl; 5 HEPES; 3 EGTA; 3 $MgCl_2$; 1 $CaCl_2$; 2 glucose; 1 Mg-ATP; 1 GTP (pH 7.2), we found that the resting membrane potential of HEK293 cells averaged -51.6 ± 1.0 mV (N = 10). Patches were held at $+10$ mV yielding a net trans-membrane voltage of -61.6 mV across the membrane patch. Channel openings were stimulated with 5 s test pulses to depolarize the membrane patch by 50 mV to -11.6 mV. Gluconate replacement depolarized HEK293 cells by ~10 mV to -39.1 ± 1.5 mV (N = 10). To compensate for the depolarization produced by gluconate, we analyzed test steps that depolarized the patch by only 40 mV rather than 50 mV. Single channel amplitude and open probability were analyzed during 5 s test pulses using Clampfit software (Axon Instruments).

Unless otherwise specified, all chemicals were obtained from Sigma Chemicals (St. Louis, MO). The criterion for statistical significance was chosen to be P<0.05 and evaluated with Student's T-test or ANOVA using GraphPad Prism 4. Variability is reported as ±SEM.

Results

Effects of Chloride Replacement on CaV1.2 Currents

α_1 subunits of CaV1.2 channels were co-expressed with EGFP, β_{2a} and $\alpha_2\delta$ subunits in HEK293 cells. Currents were measured with a ramp voltage protocol and 5 mM Ba^{2+} was used as a charge carrier to enhance currents through Ca^{2+} channels. Fitting ramp-evoked I_{Ba} with a Boltzmann function adjusted for driving force yielded a midpoint activation (V_{50}) of -10.5 ± 0.9 mV and slope factor of -8.3 ± 0.4 (N = 17; Table 1) consistent with previous reports [38]. Untransfected HEK293 cells exhibit a small endogenous I_{Ba} [39] which averaged 0.065 ± 0.006 pA/pF (N = 33), much smaller than currents in CaV1.2-transfected cells (22.0 ± 4.5 pA/pF, N = 17).

As illustrated in Fig. 1, CaV1.2 currents were strongly inhibited by replacing extracellular chloride with equimolar gluconate. Increasing the concentration of gluconate caused progressive inhibition of I_{Ba}, attaining $82.9\pm2.8\%$ (N = 28) inhibition of peak amplitude at 135 mM gluconate. Similar strong inhibition by gluconate replacement was observed when CaV1.2 currents were measured using voltage step protocols ($-76.9\pm3.7\%$, N = 8, Fig. S1). The small endogenous I_{Ba} was not significantly inhibited by gluconate replacement ($-7.2\pm5.5\%$, N = 31, P = 0.57). Fig. 1B plots the average change in I_{Ba} amplitude observed with different concentrations of gluconate. Consistent with experiments on L-type currents in vivo [8], replacing only 14 mM chloride with gluconate significantly inhibited I_{Ba}.

Inhibition by gluconate was accompanied by a negative voltage shift in I_{Ba} (Fig. 1A). At a gluconate concentration of 135 mM, V_{50} determined from the Boltzmann fit to the average I_{Ba} from 13 cells

shifted by -8.1 mV. This negative shift in V_{50} is due to effects of gluconate on membrane surface charge [11,16,18,40]. By promoting a leftward shift in the voltage-dependence of outward K^+ or Cl^- currents [9,11,14,16,18,41,42], surface charge effects also contributed to a small negative shift in the net whole cell reversal potential in some cells. To test for the possibility that changes in driving force might have significantly influenced measurements of the inhibitory effects of gluconate on peak amplitude of I_{Ba}, we analyzed effects of gluconate on the maximum conductance of I_{Ba} (G_{max}) determined from the Boltzmann function fit to the average I_{Ba} waveform. Similar to gluconate's effects on I_{Ba} amplitude, G_{max} was reduced 72% by replacing 135 mM Cl^- with equimolar gluconate. Inhibition of I_{Ba} by gluconate can enhance the contribution of residual currents to the net whole cell current. The impact of residual K^+ currents on measured changes in I_{Ba} peak amplitude appeared minimal since we observed a similar reduction in amplitude when we conducted gluconate replacement experiments using a higher concentration of TEA (60 mM; $-74.7\pm3.4\%$, N = 9, P = 0.14, unpaired t-test).

The identity of the substituting anion influenced the effects of chloride replacement. Perchlorate is a low charge density anion that has been shown to alter I_{Ba} and Ca^{2+}-mediated processes in many cell types [13,14,16,18]. By contrast with inhibitory effects of 14 mM gluconate, 14 mM perchlorate enhanced CaV1.2 (Fig. 1C). This is consistent with the enhancement of L-type I_{Ca} produced by low concentrations of perchlorate in various tissues [13,14,16]. However, higher perchlorate concentrations caused a progressive inhibition of CaV1.2 currents with almost complete inhibition achieved at a concentration of 135 mM perchlorate ($-96.8\pm0.9\%$, N = 7). To test whether this inhibitory effect was also observed with L-type Ca^{2+} channels in vivo, we recorded I_{Ca} from acutely isolated rat ventricular muscle cells and examined the effects of 135 mM perchlorate. Similar to the inhibition observed with expressed CaV1.2 channels, we found that 135 mM perchlorate inhibited the peak amplitude of I_{Ca} in ventricular muscle cells by $78.5\pm2.0\%$ (N = 6). The finding that low

Table 1. Boltzmann parameters and current densities for different channel combinations.

|	V_{50} (mV)	Slope factor	G_{max} (nS)	Current density (pA/pF)	N
CaV1.2/$\alpha_2\delta$/β_{2A}	-10.5 ± 0.9	-8.3 ± 0.4	3.2 ± 0.5	22 ± 4.5	17
CaV1.2/$\alpha_2\delta$/β_{1B}	-12.5 ± 3.1	-9.5 ± 2.0	1.8 ± 0.3	21.6 ± 6.0	6
CaV1.2/$\alpha_2\delta$/β_3	-10.6 ± 3.1	-10.9 ± 1.5	3.6 ± 1.2	16.2 ± 4.2	13
CaV1.2/$\alpha_2\delta$/β_4	-9.2 ± 3.9	-11.3 ± 0.8	1.9 ± 0.2	20 ± 5.8	5
CaV1.2/$\alpha_2\delta$	-9.6 ± 1.9	-10.7 ± 0.8	2.8 ± 1.2	8.5 ± 1.8	14
CaV1.2/β_{2A}	-4.6 ± 1.1	-9.8 ± 1.6	1.6 ± 0.7	6.0 ± 3.0	4
CaV1.2	-8.1 ± 1.6	-11.0 ± 0.5	1.9 ± 0.5	7.5 ± 1.7	6
LongNT/$\alpha_2\delta$/β_{2A}	-9.8 ± 1.8	-11.4 ± 0.8	2.1 ± 0.5	18.1 ± 5.6	13
LongNT/$\alpha_2\delta$	-8.8 ± 5.6	-13.8 ± 1.1	2.0 ± 0.7	4.4 ± 1.0	6
Δ139/$\alpha_2\delta$/β_{2A}	-16.5 ± 1.8	-10.0 ± 0.8	3.2 ± 0.7	12.5 ± 2.1	9
Δ6–20/$\alpha_2\delta$/β_{2A}	-12.6 ± 2.4	-11.0 ± 0.8	2.4 ± 0.7	11.6 ± 1.6	6
Δ6–20/$\alpha_2\delta$	-13.5 ± 0.8	-7.3 ± 1.3	1.5 ± 0.4	2.5 ± 0.5	7
Δ1665/$\alpha_2\delta$/β_{2A}	-6.5 ± 1.8	-11.9 ± 0.7	1.8 ± 0.2	3.5 ± 0.5	5
Δ1701RRQQ/$\alpha_2\delta$/β_{2A}	-11.6 ± 1.7	-10.4 ± 1.0	2.1 ± 0.3	15.6 ± 2.7	10
Δ139/Δ1665/$\alpha_2\delta$/β_{2A}	-6.8 ± 3.0	-10.2 ± 0.6	1.3 ± 0.2	12.0 ± 3.0	10
Δ1665/$\alpha_2\delta$	-4.9 ± 3.9	-10.2 ± 1.6	1.1 ± 0.3	3.7 ± 1.5	5
Δ139/Δ1700/$\alpha_2\delta$/β_{2A}	-13.6 ± 1.2	-9.6 ± 0.6	2.3 ± 0.5	9.5 ± 2.7	8

doi:10.1371/journal.pone.0008602.t001
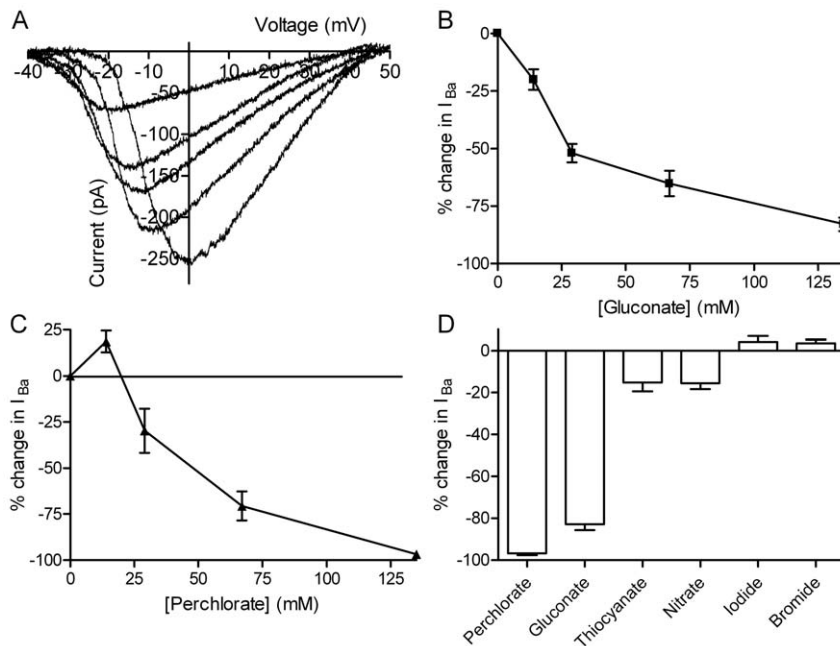
Figure 1. Effects of gluconate and other anions on CaV1.2 currents. A. CaV1.2 currents (short N-terminal isoform) were progressively inhibited by replacing increasing amounts of extracellular chloride with gluconate. 5 mM Ba^{2+} was used as a charge carrier and currents were evoked by a ramp voltage protocol (−90 to +60 mV, 0.5 mV/ms). Traces show I_{Ba} recorded in control conditions and after 2 min superfusion with solutions containing increasing concentrations of gluconate (14 mM, 28 mM, 68 mM, and 135 mM). Leak currents were removed by subtracting the ohmic conductance measured below I_{Ba} threshold. B. Increasing gluconate concentration caused a concentration-dependent increase in inhibition of the peak amplitude of CaV1.2 currents. A gluconate concentration of 14 mM caused 20.1±4.4% (N = 14) inhibition whereas 135 mM gluconate caused 82.9±2.9% inhibition (N = 28). C. Replacing 14 mM Cl^- with equimolar perchlorate increased CaV1.2 currents (18.7±5.8%, N = 6) but further increases in perchlorate concentration caused a concentration-dependent inhibition of CaV1.2 currents with −96.8±0.9% inhibition (N = 7) at a perchlorate concentration of 135 mM. D. Bar graph comparing effects of replacing 135 mM Cl^- with equimolar quantities of perchlorate (N = 7), gluconate (N = 28), thiocyanate (N = 8), nitrate (N = 9), iodide (N = 10) and bromide (N = 9). All of these experiments were performed using $\alpha_1/\beta_{2a}/\alpha_2\delta$.
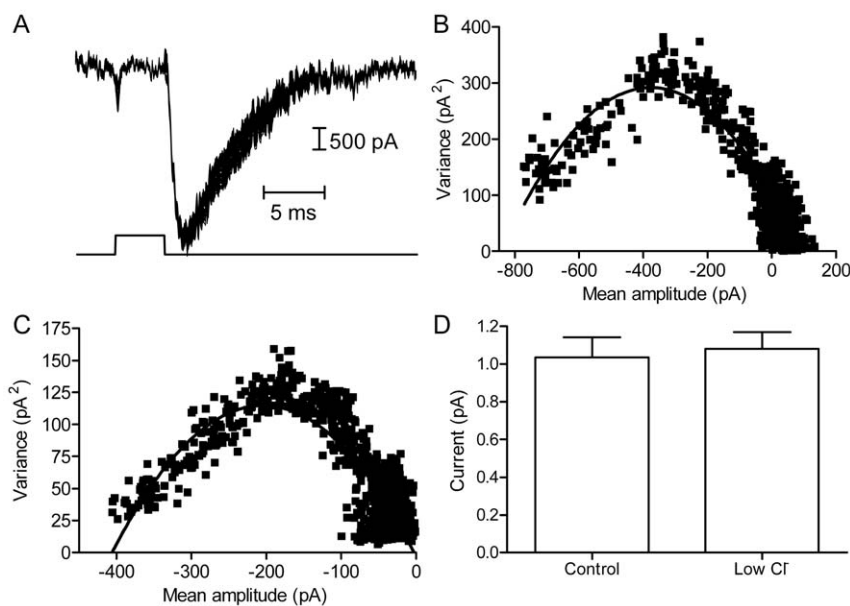doi:10.1371/journal.pone.0008602.g001

Figure 2. Replacing chloride with gluconate did not alter single channel amplitude of CaV1.2 currents. A. Overlaid traces showing a series of 100 test steps (5 ms, −70 to +50 mV). Passive membrane properties were subtracted using a P/200 protocol. B. The mean amplitude of the I_{Ba} tail current (A) was plotted against the variance at each time point (beginning at the peak inward current). The relationship between mean and inter-trial variance at different time points was fit with a parabolic function (see Methods). The best fit with this function indicates that I_{Ba} resulted from 746±21 channels with a single channel amplitude averaging −1.01±0.02 pA. C. Replacing 29 mM Cl^- with equimolar gluconate inhibited the amplitude of I_{Ba} by 48% in this cell, but the best fit parabola to the mean/variance relationship showed little change in single channel current amplitude (−1.15±0.03 pA). D. On average, lowering chloride had no significant effect on single channel current amplitude (control: −1.04±0.11 pA, N = 19; 29 mM gluconate: −1.08±0.09 pA, N = 19, P = 0.76).
doi:10.1371/journal.pone.0008602.g002

concentrations of perchlorate enhanced I_{Ba} whereas high concentrations inhibited I_{Ba} could be explained by the presence of different anion interaction sites that exhibit different affinities for perchlorate.

We tested effects of other anions to determine whether inhibition of CaV1.2 currents follows the Hofmeister series (perchlorate>iodide>nitrate>bromide~chloride), as found with L-type I_{Ca} in photoreceptors [18,40,43]. Replacing 135 mM chloride with bromide (+3.5±1.8%, N=9) produced no significant effect on CaV1.2 current amplitude (Fig. 1D). Iodide also had little effect on CaV1.2 currents (+4.1±2.8%, N=10). Nitrate replacement caused a modest but significant inhibition (−15.5±2.8%, N=9; P=0.0006). Interestingly, thiocyanate, which occupies a similar position in the Hofmeister series as perchlorate, caused only modest inhibition of −15.2±4.3% (N=8). However, this is consistent with findings that thiocyanate has little effect on I_{Ca} in ventricular muscle cells [10]. Inhibitory effects of anions on CaV1.2 thus differed somewhat from the Hofmeister sequence, following the order perchlorate>gluconate>>thiocyanate~nitrate>iodide~bromide~chloride.

Mechanisms of Anion Regulation

Previous studies have shown that the effects of anions on L-type I_{Ca} in pancreatic beta cells and retinal photoreceptors are due to changes in Ca^{2+} channel open probability and not to changes in single channel conductance [16–18]. We tested whether gluconate influences single channel current amplitude of CaV1.2 currents by using mean/variance analysis techniques. To do so, we activated I_{Ba} using a series of 100 brief test steps from −70 to +50 mV. We measured the I_{Ba} tail current after P/200 subtraction of passive membrane properties (Fig. 2A). The relationship between mean and inter-trial variance at different time points was fit with a parabolic function. In the example shown in Fig. 2B, the best fit parabolic function to the mean/variance relationship (see Methods) indicated that the tail current resulted from 746±21 channels with a single channel current amplitude averaging −1.01±0.02 pA. Lowering extracellular chloride level from 143 to 116 mM by replacement with equimolar gluconate inhibited I_{Ba} by 48% in this cell (Fig. 2C), but had little effect on single channel current amplitude (−1.15±0.03 pA, Fig. 2C). In 19 cells, lowering chloride by 29 mM through gluconate replacement produced no significant effect on single channel current amplitude (Fig. 2D).

For a more direct test of the hypothesis that intracellular anion changes alter channel open probability, we obtained cell-attached patch recordings of single CaV1.2 channels. We employed an experimental approach used previously to study anion sensitivity of single L-type Ca^{2+} channels in photoreceptor terminals [17]. The recording pipette was filled with 82 mM $BaCl_2$ to enhance
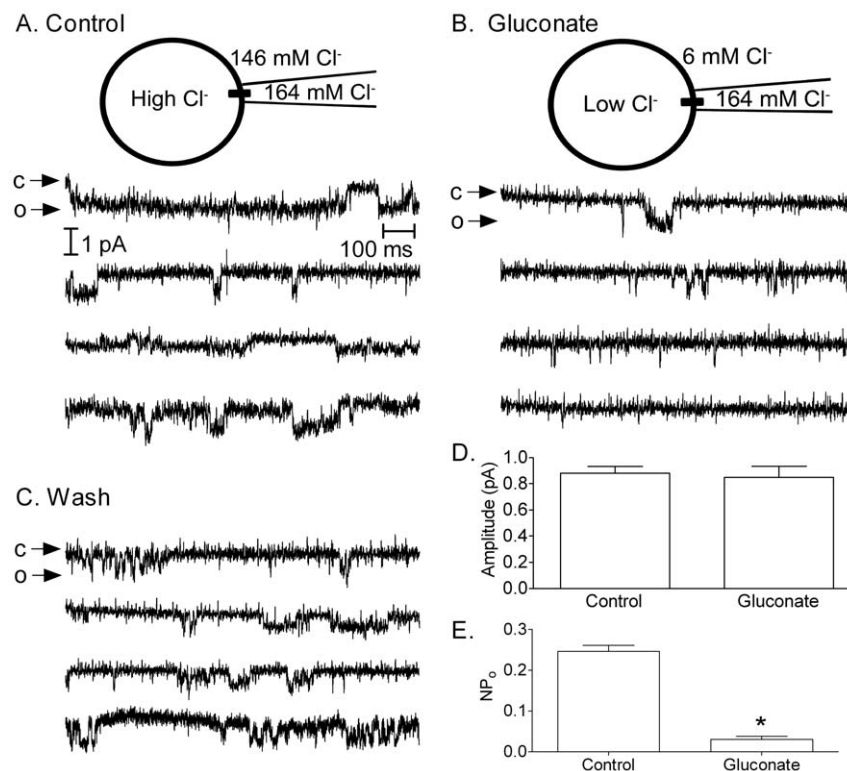

Figure 3. Gluconate replacement acts inside the cell to reduce Ca^{2+} channel open probability. CaV1.2 channel openings were recorded using the cell-attached patch configuration. Inward currents into the cell are shown as downward deflections. Panel A shows a sequence of 4 sweeps in control conditions. Panel B shows that that the number of channel openings dropped dramatically when extracellular Cl^- was replaced with gluconate (135 mM). Panel C shows that channel openings recovered after washout. The extracellular channel surface was continuously exposed to 164 mM Cl^- in the recording pipette suggesting that the reduction in channel opening are due to intracellular effects of gluconate replacement. For illustration, currents were smoothed by Butterworth filtering (8-pole, 800Hz). D. The amplitude of single channel currents was not significantly reduced by gluconate (N=7, P=0.38, paired t-test). C. Channel open probability (NP_o) was significantly reduced by gluconate replacement (N=7, P<0.0001, paired t-test). Control data were analyzed from sweeps obtained at an estimated trans-membrane potential across the patch of ~−12 mV. Gluconate sweeps were analyzed using a 10 mV more positive test pulse to compensate for the ~10 mV depolarization of HEK293 cells produced by the gluconate solution.
doi:10.1371/journal.pone.0008602.g003

the amplitude of single channel Ca^{2+} currents. Channel openings were stimulated by applying test steps (5 s) to depolarize the membrane patch to ~-12 mV (see Methods). The absence of cations other than Ba^{2+} in the pipette and the high concentration of Cl^- favoring Cl^- influx (outward current) indicate that inward channel currents were carried by Ba^{2+}. Consistent with previously reported values for L-type Ca^{2+} channels (e.g., [19,44–50]), the peak mean open probability of channel openings during 5 s test pulses averaged 0.23 ± 0.03 (N = 13) and the slope conductance determined from channel currents measured at three different test potentials averaged 19.8 ± 3.9 pS (N = 6). As illustrated in Fig. 3, replacing Cl^- with gluconate in the bathing medium caused a substantial reduction in open probability from 0.25 ± 0.01 to 0.03 ± 0.01 (N = 7, P<0.0001, paired t-test). Because the extracellular membrane surface was exposed to 164 mM Cl^- in the recording pipette, the reduction in Ca^{2+} channel openings was presumably due to changes in intracellular anion levels resulting from bath application of the gluconate solution. Consistent with an efflux of Cl^- through endogenous Cl^- channels in HEK293 cells [41], the gluconate test solution depolarized HEK293 cells by ~10 mV, from -51.6 ± 1.0 mV to -39.1 ± 1.5 mV (N = 10). To compensate for this change in membrane potential, gluconate sweeps were analyzed using a test pulse that was 10 mV more positive than the test pulse used for analysis in control conditions. However, a large reduction in the number of channel openings was observed with gluconate at all three test potentials (data not shown). The reduction in open probability could be reversed by washout of the gluconate solution (Fig. 3). Consistent with results of variance/mean analysis shown in Fig. 2, the amplitude of channel openings that occurred in the presence of the gluconate test solution did not differ significantly from openings measured in control conditions (Fig. 3B). The finding that single channel current amplitudes were unchanged by Cl^- replacement also provides further evidence that single channel currents were not the result of Cl^- channel openings. These findings confirm results of earlier studies [16,17] showing that the inhibition of I_{Ba} by gluconate replacement is due to intracellular effects of anions that cause a change in Ca^{2+} channel open probability.

Channel Regions Responsible for Anion Modulation

We used different subunit combinations and CaV1.2 mutations to analyze channel regions responsible for anion effects. Table 1 shows the best-fit Boltzmann parameters and current densities for each of the channel combinations. The figures illustrate effects of gluconate replacement on different channel combinations and plot the inhibition of peak current amplitude. Gluconate produced similar effects on both current amplitude and G_{max} (values provided in the figure legends).

Similar to the example in Fig. 1, Fig. 4A shows that replacement of chloride with gluconate (gray trace) caused a large decrease in the peak amplitude of the CaV1.2 current (rat CaV1.2 plus $\beta2a$ and $\alpha2\delta$; Fig. 4A). By contrast, omission of β subunits reduced gluconate inhibition from ~80% to $-44.2\pm1.8\%$ (CaV1.2/$\alpha2\delta$; N = 7; Figs. 4B–C). By selecting cells with large currents for the measurement of anion effects, we may have reduced differences in the amplitude of currents measured from cells with and without β subunits. Nevertheless, consistent with earlier studies [51–53], omission of β subunits greatly reduced CaV1.2 current density (Table 1). Omission of $\alpha_2\delta$ subunits also reduced current density (Table 1) but did not significantly alter gluconate inhibition of CaV1.2 currents relative to control (Figs. 4C, 4E; P = 0.51). We observed the same reduction in gluconate inhibition after simultaneously omitting both β and $\alpha_2\delta$ subunits as we did after omitting only β subunits ($50.3\pm8.1\%$ inhibition, N = 8; Fig. 4C).

These results show that at least a portion of the inhibitory effects of gluconate replacement requires the presence of β subunits. However, we found no significant difference in the effects of gluconate on CaV1.2 by comparing the different β subunits β_{1b}, β_{2a}, β_3, and β_4 (P = 0.81, ANOVA, Fig. 4C).

To identify sites of anion interactions on α_1 subunits, we used α_1 mutants created from a long N-terminal isoform of CaV1.2 derived from rabbit cardiac cells. Similar to the rat brain-derived N-terminal CaV1.2 isoform used for earlier experiments, gluconate replacement inhibited the cardiac-derived long N terminal isoform of CaV1.2 by $78.2\pm1.5\%$ (N = 16; Fig. 5A) and omitting β subunits reduced this inhibition to $50.2\pm1.1\%$ (N = 8; not shown).

Although β subunits do not bind directly to the N terminus [54], β subunit enhancement of long NT CaV1.2 currents nonetheless requires a region of the α_1 subunit N-terminus between residues AA 6–20 [33]. Expression of an $\alpha1$ subunit that was truncated at AA139 to remove this region along with most of the cytosolic portion of the N-terminus ($\Delta139$) reduced inhibition by gluconate from ~75% to $54.0\pm3.3\%$ (N = 9; Figs. 5B, D), similar to effects produced by omission of β subunits. We also tested a $\Delta6$–20 mutant in which only this critical region was deleted from the N terminus [33]. Similar to effects produced by removal of the entire
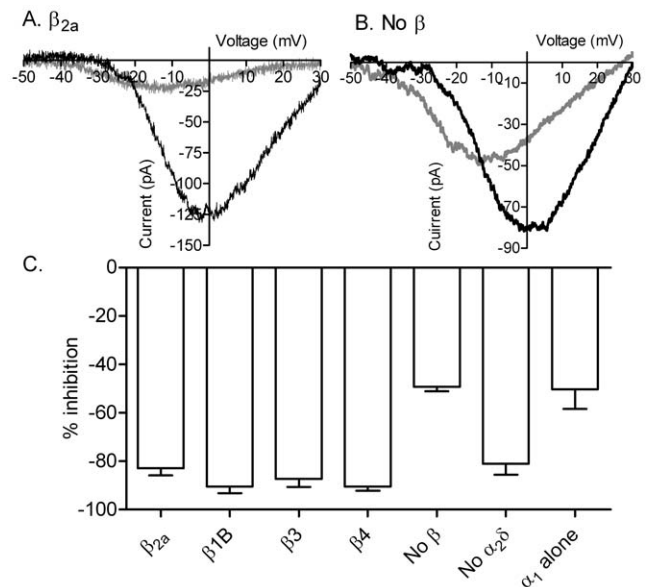

Figure 4. α1 and β subunits are involved in anion interactions with CaV1.2. A. I_{Ba} recorded from a cell expressing short N terminal CaV1.2 with $\alpha2\delta$ and $\beta2a$. Currents were recorded in control conditions (black trace) and after replacing 135 mM chloride with gluconate (gray trace). I_{Ba} was recorded using a ramp voltage protocol (-90 to $+60$ mV, 0.5 mV/ms). B. Gluconate replacement produced less inhibition of I_{Ba} when CaV1.2 was expressed without β subunits. C. Bar graph illustrating the inhibition of I_{Ba} peak amplitude produced by gluconate replacement when CaV1.2 was expressed with $\beta2a$ and $\alpha2\delta$ (reduction in amplitude: $82.9\pm2.9\%$; N = 19; reduction in G_{max}: 72.0%), without β subunits (amplitude, $-44.2\pm1.8\%$; N = 7; ΔG_{max}, -46.1%), without $\alpha2\delta$ (amplitude, $-81.0\pm4.6\%$, N = 8; ΔG_{max}, -80.0%), and after omission of both $\beta2a$ and $\alpha2\delta$ subunits (amplitude, $-50.3\pm8.1\%$; N = 8; ΔG_{max}, -49.9%). Inhibition of I_{Ba} by gluconate replacement was significantly reduced by omission of β subunits (P<0.001, unpaired t-test) or simultaneous omission of both β and $\alpha_2\delta$ subunits (P<0.001). Varying the β subunit composition had no significant effect (P = 0.81, ANOVA) on gluconate inhibition of CaV1.2 amplitude (β_{1b}, N = 7, $90.4\pm2.7\%$ inhibition of amplitude, 84.6% inhibition of G_{max}; β_3, N = 12, amplitude $-87.3\pm3.3\%$, ΔG_{max} -67.8%; β_4, N = 8, amplitude $-90.4\pm1.8\%$, ΔG_{max} -76.4%).

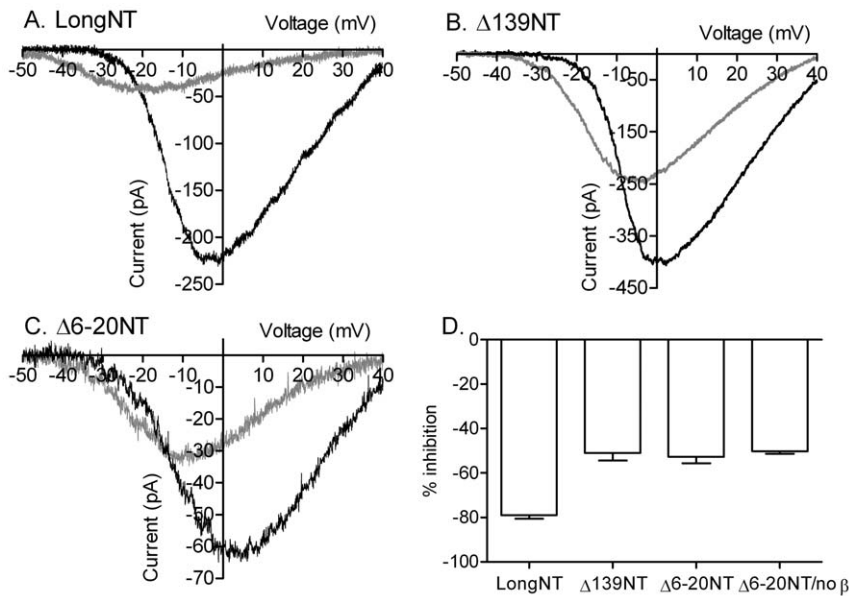doi:10.1371/journal.pone.0008602.g004

Figure 5. N-terminal regions involved in gluconate inhibition of CaV1.2. A. I_{Ba} from cardiac-derived long N-terminal CaV1.2 co-expressed with β2A and α2δ. The long N-terminal isoform showed a similar reduction in I_{Ba} after gluconate replacement (gray trace) as the short N terminal isoform of CaV1.2 used in previous figures. B. I_{Ba} from a mutant CaV1.2 in which the N-terminus was truncated at residue AA 139 (Δ139) recorded in control conditions (black trace) and after replacing chloride with gluconate (gray trace). C. I_{Ba} after deletion of residues AA 6–20 on the N-terminus (Δ6–20) from long N-terminal CaV1.2 in control (black trace) and low chloride (gray trace) conditions. D. Bar graph showing the percentage inhibition of I_{Ba} peak amplitude produced by gluconate replacement in the different experiments. Compared to the long N-terminal isoform of rabbit CaV1.2 ($-78.2\pm1.5\%$; ΔG_{max} -71.9%, N = 16), truncating the N terminus at residue 139 (Δ139: $-54.0\pm3.3\%$; ΔG_{max} -48.0%; N = 9), deletion of residues 6–20 (Δ6–20: $-53.7\pm2.6\%$; ΔG_{max} -51.6%, N = 17), or expression of Δ6–20 mutant without β subunits ($-50.2\pm1.1\%$; ΔG_{max} -44.7%, N = 8) all reduced inhibition of I_{Ba} by gluconate replacement from ~75% to ~50%.
doi:10.1371/journal.pone.0008602.g005

N terminus or omission of β subunits, gluconate inhibition was reduced to $53.7\pm2.60\%$ (N = 17) in the Δ6–20 mutant (Figs. 5C, D). Consistent with involvement of this region in β subunit-mediated anion effects, inhibition by gluconate was not reduced any further by expressing the Δ6–20 mutant without β subunits ($-50.2\pm1.1\%$, N = 8; Fig. 5D).

We then tested involvement of the C terminus in anion effects. Truncating the C terminus of rabbit CaV1.2 at AA 1700 [35] did not decrease gluconate inhibition (Figs. 6A, D) but removing only 35 additional residues by truncating the C terminus at AA 1665 [34] reduced gluconate inhibition from ~75% to $-48.1\pm2.5\%$ (N = 23; Figs. 6B, D). This indicates that there is an anion interaction site on the C terminus somewhere between residues AA 1665 and 1700.

We tested a Δ1701 truncation mutant of CaV1.2 in which two neighboring arginine residues (AA 1696 and AA 1697) residing within this anion-sensitive C-terminal region were neutralized by replacement with glutamine [36]. Inhibition of I_{Ba} by gluconate replacement was reduced in this Δ1701RRQQ mutant to $58.0\pm2.1\%$ (N = 7; Fig. 6D). This reduction in inhibition from ~75% observed with the full length channel is not due to retention of a glycine residue at position 1701 since deletion of this residue in the Δ1700 mutant yielded the same anion sensitivity as the full length channel. This result suggests that the two neighboring arginines at positions 1696 and 1697 are involved in anion effects on the C terminus.

We examined the independence of N- and C-terminal anion regulatory regions by studying a double mutant in which the N terminus was truncated at AA 139 and the C terminus truncated at AA 1665. Consistent with additive effects between the two tails, inhibition by gluconate was reduced further in the Δ139/Δ1665

double mutant to $25.4\pm6.9\%$ (N = 5; Figs. 6C–D). Inhibition by gluconate was reduced to a similar amount ($-29.4\pm5.8\%$, N = 7) when the Δ1665 mutant was expressed without β subunits (Fig. 6D). Gluconate inhibition in the Δ139/Δ1700 double mutant ($-50.8\pm4.4\%$, N = 7, Fig. 6D), which retains the anion-sensitive region on the C terminus, did not differ appreciably from gluconate inhibition observed with the Δ139 mutant.

The remaining ~25% gluconate inhibition in the Δ139/Δ1665 double mutant suggests the possibility of at least one other anion interaction site. Consistent with the existence of an additional anion interaction site, enhancement of CaV1.2 by 14 mM perchlorate ($+26.1\pm3.9\%$; N = 4, data not shown) was retained by the Δ139/Δ1665 double mutant.

Discussion

Comparison with I_{Ca} In Situ

Many of the anion effects that we found in expressed CaV1.2 channels have been observed with L-type Ca^{2+} channels *in situ*. Cardiac and skeletal muscle contractions, as well as I_{Ca} in skeletal muscle and pancreatic beta cells, are enhanced by low concentrations of perchlorate [13,14,16]. Similarly, we found that CaV1.2 currents were enhanced by low perchlorate concentrations. By contrast with low concentrations, we found that high perchlorate concentrations strongly inhibited both ventricular muscle I_{Ca} and CaV1.2 currents. Thiocyanate, which has a low charge density similar to perchlorate, did not greatly alter I_{Ca} in ventricular muscle [10] and we found that it also did not have much of an inhibitory effect on expressed CaV1.2 currents. The finding that inhibitory effects of replacing chloride with thiocyanate were much weaker than predicted from thiocyanate's position
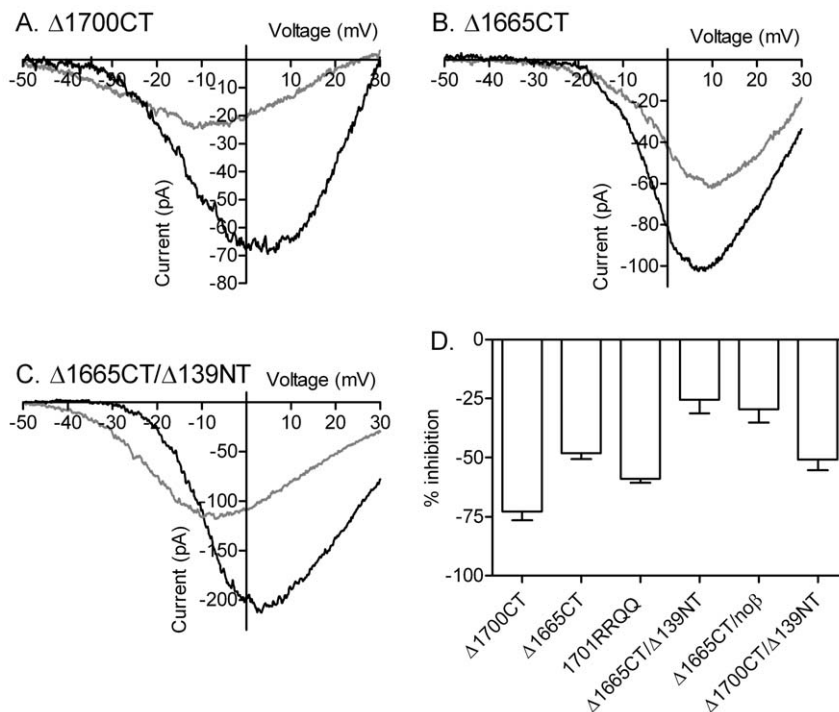
Figure 6. Contributions of the C terminus to anion sensitivity of CaV1.2 currents. A. Long NT CaV1.2 current after deletion of the C terminus at residue 1700 (Δ1700CT) in control conditions (black trace) and after replacing chloride with gluconate (gray trace). B. CaV1.2 current after deletion of the C terminus at residue 1665 (Δ1665CT) in control (black trace) and gluconate (gray trace) conditions. C. I_{Ba} from a mutant lacking both C- and N-termini (Δ1665/Δ139) in control (black trace) and gluconate (gray trace) conditions. D. Bar graph comparing the inhibition of I_{Ba} peak amplitude produced by gluconate replacement in the different mutants. Truncating the C terminus of rabbit CaV1.2 at AA 1700 (Δ1700) showed no reduction in gluconate inhibition ($-72.3\pm2.0\%$, N = 4; ΔG_{max} -73.9%) compared to full length CaV1.2. However, removing an additional 35 residues by truncating the C terminus at AA 1665 (Δ1665) reduced gluconate inhibition significantly (P<0.0001) to $48.1\pm2.5\%$ (N = 23; ΔG_{max} -45.8%). Two positively charged residues in this region were neutralized in a Δ1701 truncation mutant by replacing arginine with glutamine at AA1696 and 1697. Replacing these two residues reduced gluconate inhibition to $58.0\pm2.1\%$ (N = 7; ΔG_{max} -43.0%). Inhibition was more strongly reduced in channels lacking both C- and N-termini (Δ1665/Δ139: $-25.4\pm6.9\%$, N = 5, comparison to Δ1665 with β subunits, P<0.0011; $\Delta Gmax$ -35.4%) as well as in Δ1665 channels expressed without β subunits ($-29.4\pm5.8\%$, N = 7, comparison to Δ1665 with β subunits, P<0.003; ΔG_{max} -25.6%). Gluconate inhibition in the Δ139/Δ1700 double mutant ($-50.8\pm4.4\%$, N = 7; ΔG_{max} -41.0%) did not differ from gluconate inhibition in the Δ139 mutant. Except where specified, α1 subunits were co-expressed with α2δ and β2A.
doi:10.1371/journal.pone.0008602.g006

in the Hofmeister series could be explained by the presence of spatially restricted anion binding sites that accommodate one anion better than another.

Channel Mechanisms

The inhibition of I_{Ca} in photoreceptors produced by replacement of chloride with gluconate and the enhancement of I_{Ca} in insulin-secreting beta cells produced by low perchlorate levels have both been shown to be due to changes in open channel probability mediated at intracellular sites [16,17]. Consistent with these studies, the present results also indicate that application of gluconate test solutions reduced the open probability of single CaV1.2 channels by actions at intracellular sites. By contrast with effects on open probability, the amplitude of single CaV1.2 channel currents measured using cell-attached patch techniques or mean-variance analysis was not reduced by gluconate replacement. In photoreceptor cells, chloride imaging experiments show that application of low chloride gluconate solutions causes a reduction in intracellular Cl^- levels [17]. Similarly, we found that the gluconate solution depolarized HEK293 cells consistent with an efflux of Cl^- through endogenous Cl^- channels [41]. The reduction in open probability produced by superfusion with the gluconate solution is thus most likely due to intracellular effects of gluconate replacement since, in the cell-attached patch configu-

ration, the extracellular channel surface remains continually exposed to high Cl^- levels. Also consistent with intracellular sites of anion modulation, truncating the intracellular N and C termini of the α1 subunit substantially reduced anion sensitivity. Thus, our results confirm earlier studies on endogenous channels [16,17] showing that anions influence the amplitude of L-type Ca^{2+} currents anions by acting at intracellular sites to regulate channel open probability.

N-Terminal Interactions

Replacing 135 mM extracellular chloride with gluconate inhibited CaV1.2 currents by ~75–80%. However, omitting β subunits or deleting a short N terminal region of the α1 subunit involved in β subunit interactions (AA6–20) reduced gluconate inhibition to ~50%. β subunits attach to the intracellular loop between transmembrane domains I and II of α1 subunits [54] but residues AA6–20 of the N terminus of the long NT isoform of CaV1.2 are critically important for β subunit enhancement of channel open probability [33]. Consistent with a critical role for this region in β subunit effects, there was no additional change in gluconate inhibition when the Δ6–20 mutant was expressed without β subunits.

The only positively charged amino acid residues at physiological pH are lysine and arginine. Anion binding to these residues has

been shown to regulate many different proteins including vertebrate opsins [19], intracellular Ca^{2+} channels [20], hemoglobin [21,22], albumin [23], PDZ domains [24], K^+ channels [25,26], and kainate receptors [27]. There is also evidence that anions can influence protein function indirectly by charge shielding effects that do not require binding to specific residues [21] or by modulating the activity of serine/threonine kinases [28–30] and G proteins [31]. CaV1.2 and its accessory subunits possess numerous lysine and arginine residues. However, as illustrated by the diagram in Fig. 7, lysine and arginine residues are absent from AA 6–20 of the long N terminus of CaV1.2 suggesting that anions do not interact directly with this region. The shorter rat brain-derived CaV1.2 isoform used for some experiments lacks this N terminal sequence. Nonetheless, omission of β subunits caused a similar reduction in gluconate inhibition with both isoforms of CaV1.2. This further suggests that anions interact directly with β subunits rather than the N terminus. However, we found no difference in the effects of gluconate on CaV1.2 expressed with different β subunits suggesting that, if there is a direct interaction between anions and β subunits, it is likely to involve one of the more than 20 positively charged residues conserved among β_{1b}, β_{2a}, β_3, and β_4 subunits. Together, these results suggest that anions influence steric interactions between the N-terminus and β subunits that contribute to enhancement of CaV1.2 currents [33,55,56].

C-Terminal Interactions

Truncating the C terminus at residue AA 1665 reduced gluconate inhibition to ~50% but gluconate inhibition was not reduced in a mutation retaining an additional 35 residues on the C
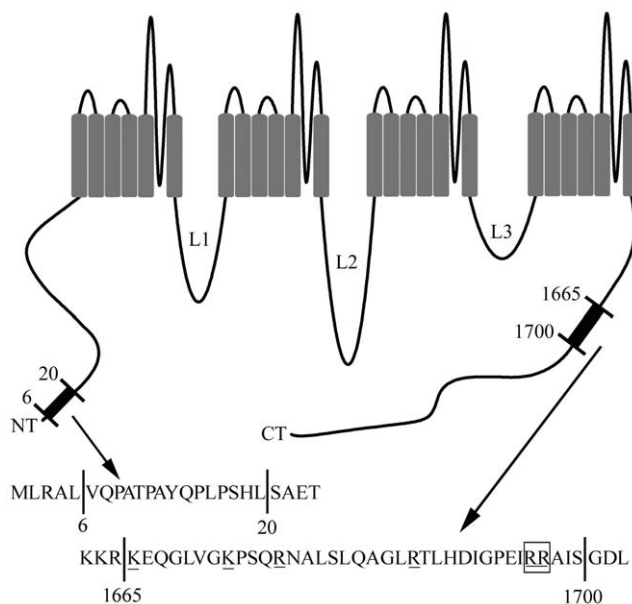

Figure 7. Diagram of the long NT CaV1.2 α_1 subunit highlighting anion-sensitive regions. Our results show that anion modulation of the long NT isoform of CaV1.2 involves the interaction between β subunits and a short N terminal region between residues AA 6–20. The absence of positively charged lysine or arginine residues in this region suggests that anions do not bind directly to this region but may instead interact with residues on the β subunit. We also identified sites of anion interaction in a C terminal region between AA 1665–1700. Two neighboring arginine residues at positions 1696 and 1697 are particularly important for these interactions.
doi:10.1371/journal.pone.0008602.g007

terminus. This indicates that residues within the short region between AA 1665 and AA 1700 are required for this aspect of gluconate's inhibitory effects. This region contains six positively charged residues (2 lysines and 4 arginines) that could potentially interact with anions (Fig. 7). Neutralizing two arginine residues at AA 1696 and AA 1697 by replacement with glutamine reduced gluconate inhibition from ~75% to ~60% suggesting that these two neighboring residues are involved in anion regulation of Ca^{2+} channel activity.

Anion effects on the C terminus were additive with anion modulation of β subunit/N terminal interactions. Truncation of either the C or N terminus alone reduced gluconate inhibition from ~75% to ~50%, whereas expression of a double mutant that lacked both termini reduced inhibition to ~25%. Gluconate inhibition was also reduced to ~25% when the C terminal truncation mutant (Δ1665) was expressed without β subunits. The residual gluconate inhibition seen in the double mutant suggests the possibility of a third anion interaction site, perhaps on the intracellular loops or more proximal tail regions of the α_1 subunit. The possibility of a third anion-interaction site is supported by the finding that the enhancement of I_{Ba} produced by low concentrations of perchlorate persists after truncation of both N and C termini. One attractive candidate for an additional anion interaction site is a cluster of positively charged residues just proximal to residue 1665 on the C terminus.

Functional Implications

The evidence that anions act primarily at the intracellular membrane surface has physiological implications since intracellular chloride levels vary more widely than extracellular chloride levels under both physiological and pathophysiological conditions [57]. For example, intracellular chloride levels fall by 20 mM during hyperpolarizing responses to light in retinal horizontal cells [58] and decrease by ≥15 mM during spontaneous action potential bursts in embryonic spinal cord neurons [59]. Reducing extracellular chloride by 14 mM with gluconate replacement inhibited CaV1.2 currents by ~20% suggesting that physiologically attainable reductions in chloride levels could have potentially significant effects on I_{Ca}. Consistent with a physiological role for anion modulation of L-type Ca^{2+} channels, chloride efflux through Ca^{2+}-activated chloride channels or chloride channels associated with glutamate transporters have both been shown to regulate the L-type I_{Ca} that controls neurotransmitter release from photoreceptor cells [17,60,61]. Similarly, chloride flux through Ca^{2+}-activated chloride channels in other tissues [62] might also potentially influence I_{Ca}. Chloride fluxes through volume-regulated anion channels cause swelling-induced changes in I_{Ca} that can stimulate insulin secretion from pancreatic beta cells as well as the contraction of cardiac and smooth muscle [63–66]. The present results suggest that, in addition to causing changes in membrane potential, swelling-induced chloride flux might exert a direct effect on I_{Ca}. Effects of intracellular chloride may also help to explain the unexpected effects of chloride channel blockers on L-type I_{Ca} [10,67].

Summary

We found that CaV1.2 currents were influenced by the presence of various anions and could be strongly inhibited by replacement of extracellular Cl^- with gluconate or perchlorate. Inhibition of I_{Ca} by gluconate replacement results from actions at the intracellular membrane surface that modulate single channel open probability but not conductance. The anion sensitivity of CaV1.2 currents involves interactions between accessory β subunits and the α1 subunit N terminus along with a short region of the α1

subunit C terminus (AA 1665–1700), particularly a pair of neighboring arginine residues at positions 1696 and 1697. The evidence that anions can regulate open probability by interactions involving both N and C terminal regions of the α_1 subunit along with the β subunit fits with the emerging view that interactions between the two tails of the calcium channel help to determine the likelihood of channel opening [35]. The strong effects of anion modulation, the sensitivity to small chloride changes, and the widespread distribution of CaV1.2 L-type Ca^{2+} channels suggest that changes in the levels of chloride and other physiological anions may be capable of influencing calcium-mediated processes in many different cell types.

Supporting Information

Figure S1 Comparison of CaV1.2 currents measured in a cell using voltage ramps (A, 0.5 mV/ms) and steady currents during steps (B, 100 ms, 10 mV increments) in control conditions (black trace in A, circles in B) and following substitution of chloride with gluconate (gray trace in A, triangles in B).
Found at: doi:10.1371/journal.pone.0008602.s001 (1.00 MB TIF)

Author Contributions

Conceived and designed the experiments: WBT. Performed the experiments: NB GJR. Analyzed the data: NB WBT. Contributed reagents/materials/analysis tools: NK ND DDPS NF. Wrote the paper: WBT.

References

1. Lipscombe D, Helton TD, Xu W (2004) L-type calcium channels: The low down. J Neurophysiol 92: 2633–2641.
2. Mears D (2004) Regulation of insulin secretion in islets of Langerhans by Ca(2+)channels. J Membr Biol 200: 57–66.
3. Bodi I, Mikala G, Koch SE, Akhter SA, Schwartz A (2005) The L-type calcium channel in the heart: The beat goes on. J Clin Invest 115: 3306–3317.
4. Heidelberger R, Thoreson WB, Witkovsky P (2005) Synaptic transmission at retinal ribbon synapses. Prog Retin Eye Res 24: 682–720.
5. Kobayashi T, Yamada Y, Fukao M, Tsutsuura M, Tohse N (2007) Regulation of Cav1.2 current: Interaction with intracellular molecules. J Pharmacol Sci 103: 347–353.
6. Kurokawa J (2007) Compartmentalized regulations of ion channels in the heart. Biol Pharm Bull 30: 2231–2237.
7. Bell DC, Butcher AJ, Berrow NS, Page KM, Brust PF, et al. (2001) Biophysical properties, pharmacology, and modulation of human, neuronal L-type (alpha(1D), Ca(V)1.3) voltage-dependent calcium currents. J Neurophysiol 85: 816–827.
8. Thoreson WB, Nitzan R, Miller RF (1997) Reducing extracellular Cl^- suppresses dihydropyridine-sensitive Ca^{2+} currents and synaptic transmission in amphibian photoreceptors. J Neurophysiol 77: 2175–2190.
9. Garcia L, Fahmi M, Prevarskaya N, Dufy B, Sartor P (1997) Modulation of voltage-dependent Ca^{2+} conductance by changing Cl^- concentration in rat lactotrophs. Am J Physiol 272: C1178–85.
10. Zhou SS, Gao Z, Dong L, Ding YF, Zhang XD, et al. (2002) Anion channels influence ECC by modulating L-type Ca(2+) channel in ventricular myocytes. J Appl Physiol 93: 1660–1668.
11. Delay M, Garcia DE, Sanchez JA (1990) The effects of lyotropic anions on charge movement, calcium currents and calcium signals in frog skeletal muscle fibres. J Physiol 425: 449–469.
12. Fry CH, Griffiths H, Hall SK (1993) Actions of extracellular chloride ion substitution on contractility of isolated ventricular myocardium. Cardiovasc Res 27: 856–860.
13. Gallant EM, Taus NS, Fletcher TF, Lentz LR, Louis CF, et al. (1993) Perchlorate potentiation of excitation-contraction coupling in mammalian skeletal muscles. Am J Physiol 264: C559–67.
14. Ma J, Anderson K, Shirokov R, Levis R, Gonzalez A, et al. (1993) Effects of perchlorate on the molecules of excitation-contraction coupling of skeletal and cardiac muscle. J Gen Physiol 102: 423–448.
15. Thoreson WB, Miller RF (1996) Removal of extracellular chloride suppresses transmitter release from photoreceptor terminals in the mudpuppy retina. J Gen Physiol 107: 631–642.
16. Larsson-Nyren G, Sehlin J, Rorsman P, Renstrom E (2001) Perchlorate stimulates insulin secretion by shifting the gating of L-type Ca^{2+} currents in mouse pancreatic β-cells towards negative potentials. Pflugers Arch 441: 587–595.
17. Thoreson WB, Nitzan R, Miller RF (2000) Chloride efflux inhibits single calcium channel open probability in vertebrate photoreceptors: Chloride imaging and cell-attached patch-clamp recordings. Vis Neurosci 17: 197–206.
18. Thoreson WB, Stella SL (2000) Anion modulation of calcium current voltage dependence and amplitude in salamander rods. Biochim Biophys Acta 1464: 142–150.
19. Wang Z, Asenjo AB, Oprian DD (1993) Identification of the Cl(−)-binding site in the human red and green color vision pigments. Biochemistry 32: 2125–2130.
20. Saito M, Hanson PI, Schlesinger P (2007) Luminal chloride-dependent activation of endosome calcium channels: Patch clamp study of enlarged endosomes. J Biol Chem 282: 27327–27333.
21. Perutz MF, Fermi G, Poyart C, Pagnier J, Kister J (1993) A novel allosteric mechanism in haemoglobin. Structure of bovine deoxyhaemoglobin, absence of specific chloride-binding sites and origin of the chloride-linked bohr effect in bovine and human haemoglobin. J Mol Biol 233: 536–545.
22. Numoto N, Nakagawa T, Kita A, Sasayama Y, Fukumori Y, et al. (2008) Structural basis for the heterotropic and homotropic interactions of invertebrate giant hemoglobin. Biochemistry 47: 11231–11238.
23. Scatchard G, Coleman JS, Shen AL (1957) Physical chemistry of protein solutions. VII. the binding of some small anions to serum albumin. J Am Chem Soc 79: 12–20.
24. Chi CN, Engstrom A, Gianni S, Larsson M, Jemth P (2006) Two conserved residues govern the salt and pH dependencies of the binding reaction of a PDZ domain. J Biol Chem 281: 36811–36818.
25. Bekar LK, Walz W (1999) Evidence for chloride ions as intracellular messenger substances in astrocytes. J Neurophysiol 82: 248–254.
26. Bekar LK, Walz W (2002) Intracellular chloride modulates A-type potassium currents in astrocytes. Glia 39: 207–216.
27. Plested AJ, Mayer ML (2007) Structure and mechanism of kainate receptor modulation by anions. Neuron 53: 829–841.
28. Lytle C, Forbush B (1996) Regulatory phosphorylation of the secretory Na-K-Cl cotransporter: Modulation by cytoplasmic cl. Am J Physiol 270: C437–48.
29. Dowd BF, Forbush B (2003) PASK (proline-alanine-rich STE20-related kinase), a regulatory kinase of the na-K-cl cotransporter (NKCC1). J Biol Chem 278: 27347–27353.
30. Ponce-Coria J, San-Cristobal P, Kahle KT, Vazquez N, Pacheco-Alvarez D, et al. (2008) Regulation of NKCC2 by a chloride-sensing mechanism involving the WNK3 and SPAK kinases. Proc Natl Acad Sci U S A 105: 8458–8463.
31. Higashijima T, Ferguson KM, Sternweis PC (1987) Regulation of hormone-sensitive GTP-dependent regulatory proteins by chloride. J Biol Chem 262: 3597–3602.
32. Snutch TP, Tomlinson WJ, Leonard JP, Gilbert MM (1991) Distinct calcium channels are generated by alternative splicing and are differentially expressed in the mammalian CNS. Neuron 7: 45–57.
33. Kanevsky N, Dascal N (2006) Regulation of maximal open probability is a separable function of Ca(v)beta subunit in L-type Ca^{2+} channel, dependent on NH2 terminus of alpha1C (Ca(v)1.2alpha). J Gen Physiol 128: 15–36.
34. Perets T, Blumenstein Y, Shistik E, Lotan I, Dascal N (1996) A potential site of functional modulation by protein kinase A in the cardiac Ca^{2+} channel alpha 1C subunit. FEBS Lett 384: 189–192.
35. Ivanina T, Blumenstein Y, Shistik E, Barzilai R, Dascal N (2000) Modulation of L-type Ca^{2+} channels by gbeta gamma and calmodulin via interactions with N and C termini of alpha 1C. J Biol Chem 275: 39846–39854.
36. Hulme JT, Yarov-Yarovoy V, Lin TW, Scheuer T, Catterall WA (2006) Autoinhibitory control of the CaV1.2 channel by its proteolytically processed distal C-terminal domain. J Physiol 576: 87–102.
37. Rozanski GJ, Xu Z (2002) Glutathione and K(+) channel remodeling in postinfarction rat heart. Am J Physiol Heart Circ Physiol 282: H2346–55.
38. Catterall WA, Perez-Reyes E, Snutch TP, Striessnig J (2005) International union of pharmacology. XLVIII. Nomenclature and structure-function relationships of voltage-gated calcium channels. Pharmacol Rev 57: 411–425.
39. Berjukow S, Doring F, Froschmayr M, Grabner M, Glossmann H, et al. (1996) Endogenous calcium channels in human embryonic kidney (HEK293) cells. Br J Pharmacol 118: 748–754.
40. McLaughlin S, Bruder A, Chen S, Moser C (1975) Chaotropic anions and the surface potential of bilayer membranes. Biochim Biophys Acta 394: 304–313.
41. Zhu G, Zhang Y, Xu H, Jiang C (1998) Identification of endogenous outward currents in the human embryonic kidney (HEK 293) cell line. J Neurosci Methods 81: 73–83.
42. Dani JA, Sanchez JA, Hille B (1983) Lyotropic anions. Na channel gating and Ca electrode response. J Gen Physiol 81: 255–281.

43. Collins KD (1997) Charge density-dependent strength of hydration and biological structure. Biophys J 72: 65–76.

44. Fox AP, Nowycky MC, Tsien RW (1987) Single-channel recordings of three types of calcium channels in chick sensory neurones. J Physiol 394: 173–200.

45. Sala S, Matteson DR (1990) Single-channel recordings of two types of calcium channels in rat pancreatic beta-cells. Biophys J 58: 567–571.

46. O'Dell TJ, Alger BE (1991) Single calcium channels in rat and guinea-pig hippocampal neurons. J Physiol 436: 739–767.

47. Slesinger PA, Lansman JB (1991) Inactivating and non-inactivating dihydropyr-idine-sensitive Ca^{2+} channels in mouse cerebellar granule cells. J Physiol 439: 301–323.

48. McDonald TF, Pelzer S, Trautwein W, Pelzer DJ (1994) Regulation and modulation of calcium channels in cardiac, skeletal, and smooth muscle cells. Physiol Rev 74: 365–507.

49. Colecraft HM, Alseikhan B, Takahashi SX, Chaudhuri D, Mittman S, et al. (2002) Novel functional properties of Ca(2+) channel beta subunits revealed by their expression in adult rat heart cells. J Physiol 541: 435–452.

50. Doering CJ, Hamid J, Simms B, McRory JE, Zamponi GW (2005) Cav1.4 encodes a calcium channel with low open probability and unitary conductance. Biophys J 89: 3042–3048.

51. Herzig S, Khan IF, Grundemann D, Matthes J, Ludwig A, et al. (2007) Mechanism of Ca(v)1.2 channel modulation by the amino terminus of cardiac beta2-subunits. FASEB J 21: 1527–1538.

52. Richards MW, Butcher AJ, Dolphin AC (2004) Ca^{2+} channel beta-subunits: Structural insights AID our understanding. Trends Pharmacol Sci 25: 626–632.

53. Bichet D, Cornet V, Geib S, Carlier E, Volsen S, et al. (2000) The I–II loop of the Ca^{2+} channel alpha1 subunit contains an endoplasmic reticulum retention signal antagonized by the beta subunit. Neuron 25: 177–190.

54. Pragnell M, De Waard M, Mori Y, Tanabe T, Snutch TP, et al. (1994) Calcium channel beta-subunit binds to a conserved motif in the I–II cytoplasmic linker of the alpha 1-subunit. Nature 368: 67–70.

55. Takahashi SX, Miriyala J, Colecraft HM (2004) Membrane-associated guanylate kinase-like properties of beta-subunits required for modulation of voltage-dependent Ca^{2+} channels. Proc Natl Acad Sci U S A 101: 7193–7198.

56. McGee AW, Nunziato DA, Maltez JM, Prehoda KE, Pitt GS, et al. (2004) Calcium channel function regulated by the SH3-GK module in beta subunits. Neuron 42: 89–99.

57. De Koninck Y (2007) Altered chloride homeostasis in neurological disorders: A new target. Curr Opin Pharmacol 7: 93–99.

58. Djamgoz MB, Laming PJ (1987) Micro-electrode measurements and functional aspects of chloride activity in cyprinid fish retina: Extracellular activity and intracellular activities of L- and C-type horizontal cells. Vision Res 27: 1481–1489.

59. Chub N, O'Donovan MJ (2001) Post-episode depression of GABAergic transmission in spinal neurons of the chick embryo. J Neurophysiol 85: 2166–2176.

60. Rabl K, Bryson EJ, Thoreson WB (2003) Activation of glutamate transporters in rods inhibits presynaptic calcium currents. Vis Neurosci 20: 557–566.

61. Thoreson WB, Bryson EJ, Rabl K (2003) Reciprocal interactions between calcium and chloride in rod photoreceptors. J Neurophysiol 90: 1747–1753.

62. Hartzell C, Putzier I, Arreola J (2005) Calcium-activated chloride channels. Annu Rev Physiol 67: 719–758.

63. Best L, Sheader EA, Brown PD (1996) A volume-activated anion conductance in insulin-secreting cells. Pflugers Arch 431: 363–370.

64. Drews G, Zempel G, Krippeit-Drews P, Britsch S, Busch GL, et al. (1998) Ion channels involved in insulin release are activated by osmotic swelling of pancreatic β-cells. Biochim Biophys Acta 1370: 8–16.

65. Sheader EA, Brown PD, Best L (2001) Swelling-induced changes in cytosolic [Ca^{2+}] in insulin-secreting cells: A role in regulatory volume decrease? Mol Cell Endocrinol 181: 179–187.

66. Best L (2005) Glucose-induced electrical activity in rat pancreatic beta-cells: Dependence on intracellular chloride concentration. J Physiol 568: 137–144.

67. Doughty JM, Miller AL, Langton PD (1998) Non-specificity of chloride channel blockers in rat cerebral arteries: Block of the L-type calcium channel. J Physiol 507: 433–439.